Nanochem Res 9(2): 91-102, Spring 2024

RESEARCH PAPER

Assessing the Efficacy of Gelatin Composite 3D Scaffolds in Cardiovascular Tissue Engineering: An In Vitro Study

Mohammad Mahdi Safikhani [1], Azadeh Asefnejad[1*], Rouhollah Mehdinavaz Aghdam [2], Sadegh Rahmati [1]

[1] Department of Biomedical Engineering, Science and Research Branch, Islamic Azad University, Tehran, Iran

[2] School of Metallurgy and Materials Engineering, College of Engineering, University of Tehran, Tehran, Iran

ARTICLE INFO

Article History:
Received 18 January 2024
Accepted 20 March 2024
Published 15 April 2024

Keywords:
3D printing
Scaffold
Drug Release
Heparin
Heart tissue engineering
Gelatin

ABSTRACT

This research aimed to investigate the potential of combining tissue engineering with conventional treatment methods to address cardiovascular diseases (CVD). The study focused on designing and 3D printing polymeric scaffolds using a composition of sodium alginate/hyaluronic acid/gelatin (SA/HA/Gel), incorporating heparin as a cardiovascular drug. Scaffolds were printed at different angles (30°, 45°, 60°, and 90°) to assess their physical properties. Various analyses, including scanning electron microscopy (SEM), examined factors such as swelling, porosity, degradability, contact angle, and surface morphology. Chemical changes were evaluated using Fourier-transform infrared (FTIR) testing. Biocompatibility was assessed through cell adhesion and survival rate analyses using L929 cells. Results showed that higher contact angles increased porosity (42-60%) and improved mechanical properties (47 MPa to 85 MPa). Swelling and contact angle were minimally affected by the printing angle. The release model coefficients and diffusion coefficient varied with the contact angle, suggesting alterations in the drug release mechanism. The controlled release rate of heparin aligned with scaffold degradation, ensuring efficient delivery during tissue repair. Biological evaluation demonstrated satisfactory cell adhesion, biocompatibility, and absence of toxicity in the 3D-printed scaffolds. However, altering the printing angle could modify biological properties due to changes in scaffold characteristics. This study confirms that 3D-printed SA/HA/Gel scaffolds incorporating heparin exhibit desirable physicochemical and biological attributes, making them suitable for drug release systems in cardiovascular tissue applications.

How to cite this article
NAME N. Assessing the Efficacy of Gelatin Composite 3D Scaffolds in Cardiovascular Tissue Engineering: An In Vitro Study. Nanochem Res, 2024; 9(2):91-102. DOI: 10.22036/ncr.2024.02.002

INTRODUCTION

Tissue engineering aims to regenerate and repair damaged tissues by utilizing cells, biomaterials, and appropriate biochemical and physical factors. Scaffolds are essential components in tissue engineering as they provide a supportive structure for cell attachment, proliferation, and new tissue formation [1-4]. Ideal scaffolds should possess suitable mechanical properties, biocompatibility, biodegradability, porosity, and surface chemistry to mimic the natural extracellular matrix. Gelatin and chitosan are biocompatible and biodegradable polymers commonly used in biomedical applications. However, their mechanical properties require improvement for tissue engineering scaffolds. Zinc oxide (ZnO) nanoparticles are known for their antimicrobial properties and safety [5-7]. Three-dimensional (3D) printing enables the fabrication of scaffolds with controlled architectures and intricate designs not easily achievable with traditional methods. This study focuses on developing composite scaffolds using gelatin, chitosan, and zinc oxide nanoparticles for bone

* Corresponding Author Email: *asefnejad@srbiau.ac.ir*

tissue engineering via 3D printing. The scaffolds will undergo characterization to assess their physical, mechanical, and biological properties. The hypothesis is that the addition of zinc oxide nanoparticles will enhance the mechanical strength of the gelatin/chitosan scaffolds [8-11]. Additionally, 3D printing will enable the creation of scaffolds with appropriate porosity and pore interconnectivity necessary for tissue regeneration. Ultimately, this research explores the potential of utilizing a composite system of natural polymers and nanoparticles, combined with 3D printing, in bone tissue engineering applications. Atherosclerosis is a complex inflammatory disease characterized by the buildup of plaque in arterial walls, leading to various cardiovascular complications [4]. Salisbury and Bronas (2014) highlighted the contribution of inflammation and the immune system to the etiology of atherosclerosis [5]. The global burden of atherothrombotic disease necessitates a deeper understanding of the epidemiology and risk factors associated with atherosclerosis [6]. Fruchart et al. (2004) emphasized the identification of new risk factors and the importance of patient risk assessment [7]. In addition to traditional risk factors, lifestyle factors also play a significant role in the development of high-risk atherosclerosis [8]. Traditional Chinese medicine has been explored as a potential treatment approach for atherosclerosis, prompting the need for further investigation [9]. Tissue engineering techniques offer promising avenues for cardiovascular disease research, including the emulation of early atherosclerosis in vascular microphysiological systems [10]. Among these techniques, 3D bioprinting has emerged as a cutting-edge technology for creating functional vascular channels and complex tissue structures [11].

The utilization of 3D printing technologies for scaffold fabrication holds great promise in cardiovascular tissue engineering. Ozbolat and Hospodiuk (2016) provided an overview of extrusion-based bioprinting and its current advances and future perspectives [13]. The combination of sodium alginate/hyaluronic acid/gelatin (SA/HA/Gel) in composite scaffolds, incorporating heparin as a cardiovascular drug, presents a novel approach for drug release systems [12]. Atherosclerosis, a chronic vascular disease, occurs when substances such as fat, calcium, blood, and others accumulate in the walls of blood vessels, forming atheromatous plaques. These plaques narrow and block the vessels, leading to severe complications like heart attacks and strokes if they rupture or travel through the bloodstream. Atherosclerosis is influenced by a combination of genetic and environmental factors, including age, gender, family history, smoking, high blood pressure, diabetes, high blood lipids, obesity, and lack of physical activity. The disease involves vessel wall damage, inflammation, plaque formation, and accumulation of inflammatory cells. Atherosclerosis is a significant cause of global mortality, with environmental factors and genetics playing crucial roles in its prevalence [12-16]. 3D printing is an emerging manufacturing technology that enables the creation of three-dimensional objects by depositing successive layers of materials. It operates by using three-dimensional data to produce objects in a linear or layer-by-layer fashion. In the field of 3D printing, a three-dimensional model of the desired object is generated and subsequently physically realized by the 3D printer. This technology is actively utilized by specialists and researchers across various disciplines, including biomedicine, tissue engineering, and the production of medical components [17-19]. In tissue engineering, 3D printing has become a pivotal step due to its ability to precisely fabricate and shape biological materials. By harnessing 3D printing, it becomes possible to produce intricate structures with high accuracy and intricate designs. This technological advancement enables the construction of robust tissue constructs, leading to improved disease treatment and tissue regeneration [19-22]. Heparin, a potent anticoagulant, is employed in the treatment of cardiovascular diseases such as atherosclerosis. Its inclusion in 3D scaffolds is based on its anticoagulant properties and its beneficial effects in tissue regeneration and the management of atherosclerosis [22-25]. Heparin serves several important purposes, including its role as an anticoagulant. By preventing platelet accumulation and blood clot formation, heparin enhances cardiovascular function. In the context of atherosclerosis, blood clots can impede blood flow from the heart by obstructing blood vessels, leading to severe complications such as heart attacks or strokes [26-27]. The utilization of heparin in 3D scaffolds can mitigate the risk of blood clot formation and the subsequent blockage of blood vessels [28-29]. Heparin, a potent anticoagulant, exhibits various beneficial properties when incorporated into 3D scaffolds for the treatment of atherosclerosis. Alongside its anticoagulant effects,

heparin also possesses anti-inflammatory properties that can help control inflammation and reduce the formation of atheromatous plaques, thereby improving the vascular condition. Moreover, heparin in 3D scaffolds demonstrates angiogenic properties, stimulating the growth of new blood vessels and enhancing blood supply to damaged tissues. Another advantage of heparin is its ability to degrade and be absorbed, facilitating tissue regeneration processes and allowing for precise control over the amount of heparin incorporated into the scaffold. Sodium alginate, hyaluronic acid, and gelatin are important materials in 3D printing due to their unique mechanical, structural, and biocompatible properties. Combining these materials with heparin loading in the 3D scaffold can yield superior results in the treatment of atherosclerosis. The synergistic interactions among these materials enhance the mechanical and structural properties of the scaffold and promote cellular interaction, tissue growth, degradation, and repair processes. Utilizing a 3D printer and the combination of sodium alginate, hyaluronic acid, gelatin, and heparin can significantly enhance the performance and efficiency of 3D structures, advancing the treatment of atherosclerosis and improving patients' quality of life. This research has the potential to contribute to advancements in the field of atherosclerosis treatment. This research study aims to assess the efficacy of gelatin composite 3D scaffolds in cardiovascular tissue engineering through the design and 3D printing of polymeric scaffolds using a composition of sodium alginate/hyaluronic acid/gelatin (SA/HA/Gel) incorporating heparin. The study seeks to evaluate the physical, mechanical, and biological properties of the scaffolds, including swelling, porosity, degradability, contact angle, surface morphology, and biocompatibility. Additionally, the influence of different print angles (30°, 45°, 60°, and 90°) on the scaffold properties will be investigated. The research will involve chemical analysis using Fourier-transform infrared (FTIR) testing to identify any compositional changes caused by printing. Furthermore, the study will analyze the drug release kinetics of heparin from the scaffolds and its correlation with scaffold degradation. The ultimate objective is to determine the suitability of the gelatin composite 3D scaffolds for cardiovascular tissue engineering applications based on their physicochemical and biological attributes, thereby contributing to advancements in the treatment of cardiovascular diseases.

EXPERIMENTAL

Materials and Methods

The main objective of scaffold design is to enable successful printing by considering parameters such as pore size, wall size, porosity shape, and scaffold height, while also taking into account the printer's capabilities. Solid works software was selected for its user-friendly interface, ease of learning, and compatibility with material and layer size requirements. Following the finalization of the scaffold design, bio ink was prepared using three polymers: alginate, hyaluronic acid, and gelatin. Each polymer was optimized based on its desired properties and suitability for printing. Gelatin was dissolved in deionized water, followed by stirring to achieve a homogeneous solution. Similarly, hyaluronic acid was dissolved separately in deionized water and added gradually to the gelatin solution while stirring. An 8% weight solution of alginate was prepared separately and added to the gelatin/hyaluronic acid solution, ensuring complete dissolution through extended stirring. The proportions of the solutions were adjusted considering the printing conditions and solution concentration. Crosslinking was facilitated by adding calcium chloride drop by drop to the samples, followed by stirring. Subsequently, various tests were conducted to evaluate the optimal polymer concentration and the printability of the designed gel. Rheological measurements were conducted using a rheometer with parallel plates to investigate the viscoelastic behavior of 3D printed scaffolds.

The tests were performed at 37°C, a standard temperature for biological studies, to simulate the biological environment. Gel content in the samples was determined by drying the gels in a freeze dryer for 48 hours, followed by weighing and recording their initial weight (W1). The dried hydrogels were then immersed in water at 60°C for 48 hours. Water absorption and swelling ability were assessed by weighing the samples and recording their dry weight (W0), followed by immersion in phosphate buffered saline (PBS). Dynamic oscillatory stress was applied to assess the linear viscoelastic behavior of the scaffolds at a frequency of 1 rad/s. Frequency tests were performed in the range of 10-1 rad/s to evaluate the storage modulus (G') and loss modulus (G") of the hydrogels. These measurements provided insights into the

rheological behavior of the scaffolds in response to mechanical actions and frequency changes. The gel extracts' biocompatibility and cell survival rate were evaluated using the MTT test at 24 and 72 hours after treatment. SEM was employed using a Leica360-S Stereoscan Cambridge model to examine the microstructure of the scaffolds. Image KLONK software (version 11.2.0. Edition) with the Light Measurement feature was utilized to assess pore size in different scaffold images. The biodegradability rate of gels in a phosphate buffered saline solution was investigated by dissolving phosphate buffered saline powder in water to prepare the solution.

Morphological analysis

This study focuses on fabricating scaffolds using 3D printing technology and evaluating their surface morphology. The scaffolds exhibited a smooth and uniform structure, indicating the high precision of the 3D printing process. The incorporation of polyethylene amine (PEI) in the scaffolds improved their physical properties, such as reduced swelling and slower degradation. However, higher concentrations of PEI slightly decreased cell survival rates. The scaffolds also had porous structures and intact polymer filaments, facilitating material flow and exchange.

Fig. 1 illustrates the various print angles employed in the study, specifically G1 (30°), G2 (45°), G3 (60°), and G4 (90°). These angles were chosen to investigate the influence of print angle on the resulting scaffold morphology and properties. By examining the scaffolds fabricated at different angles, a comprehensive understanding of the relationship between print angle and scaffold characteristics can be obtained. Print angle plays a crucial role in determining the overall architecture and porosity of 3D printed scaffolds. A smaller print angle, such as 30° (G1), leads to a denser structure with reduced porosity. This is because the layers are stacked more closely together, resulting in limited space for pore formation. On the other hand, a larger print angle, such as 90° (G4), tends to produce a scaffold with increased porosity. The layers are more spread out, allowing for the formation of larger and more interconnected pores. The intermediate print angles, 45° (G2) and 60° (G3), represent a balance between porosity and structural integrity. These angles can provide a compromise between the need for sufficient porosity to facilitate cell infiltration and nutrient exchange and the requirement for mechanical stability. Scaffold porosity is a critical factor in tissue engineering applications as it affects cell adhesion, migration, and proliferation. An optimal porosity level promotes cell infiltration and the formation of functional tissues, while maintaining the necessary mechanical support. By

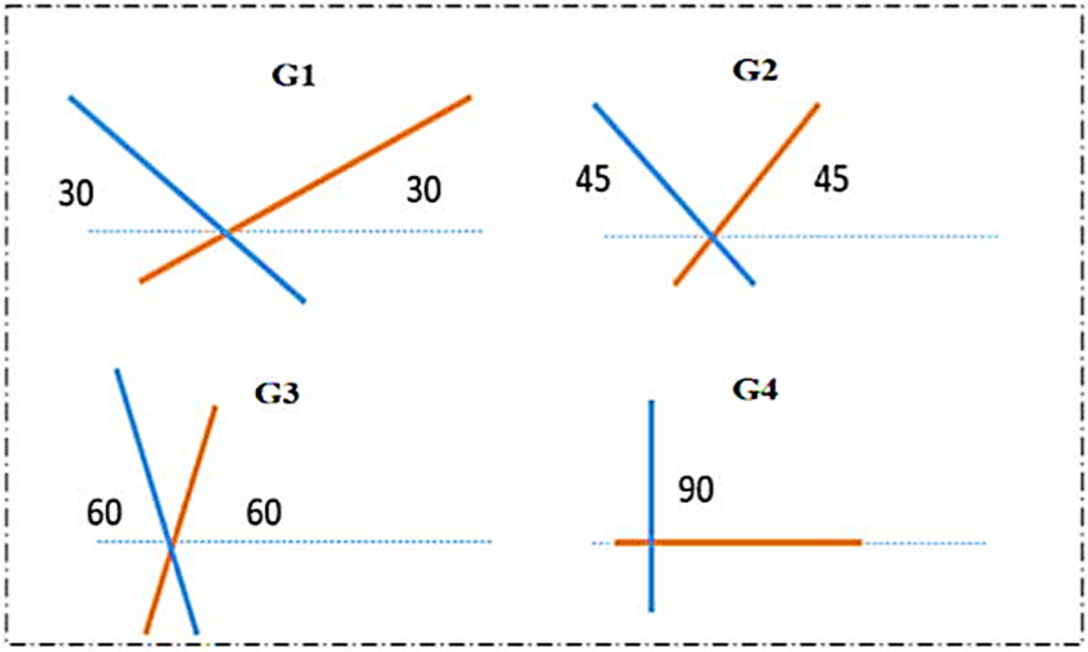

Fig. 1. Different print angles G1 (30°), G2 (45°), G3 (60°), G4 (90°)

examining the scaffolds fabricated at different print angles, the study aims to identify the print angle that yields scaffolds with desirable properties for tissue engineering applications. These properties include adequate porosity, appropriate pore size and interconnectivity, and mechanical strength. The findings from this investigation will contribute to the development of optimized 3D printing parameters and scaffold designs, enabling the fabrication of scaffolds with tailored properties based on specific tissue engineering requirements.

Porosity percentage

The findings of this study demonstrate that the porosity percentage of 3D printed scaffolds significantly increases with higher printing angles. Increasing the printing angle from 30° to 90° resulted in a porosity percentage increase from 45% to 62%. Porosity is a crucial characteristic in tissue engineering structures, particularly for medical applications, as it facilitates cell penetration and biological activity within the scaffolds. Higher porosity allows for greater empty spaces between polymer structures, enabling the penetration of biological materials and cell circulation. Conversely, reducing the printing angle brings the printed filaments closer together, resulting in reduced porosity.

RESULTS AND DISCUSSION

Bioprinting techniques have emerged as a promising approach for fabricating complex three-dimensional (3D) structures with precise control over the spatial arrangement of cells and biomaterials [26]. The use of hydrogels as bio-inks has gained significant attention in bioprinting due to their resemblance to the native extracellular matrix (ECM) and their ability to support cell survival and function [27]. However, to enhance the functionality and therapeutic potential of bio-printed constructs, the incorporation of bioactive molecules, such as heparin, is being explored. Heparin, a sulfated glycosaminoglycan, is well-known for its anticoagulant properties [29]. In the context of tissue engineering, heparin has shown promise in promoting angiogenesis [32], reducing inflammation [31], and providing sustained drug delivery [28]. Kimicata et al. developed a 3D printed mask with a heparin-loaded interlayer for vascular tissue engineering applications, demonstrating the potential of heparin in long-term drug delivery to enhance tissue regeneration [28]. In addition to its therapeutic effects, the choice of scaffold material is critical for successful tissue engineering. Poly(ε-caprolactone) (PCL) is a commonly used biocompatible polymer due to its favorable mechanical properties and biodegradability. Xing et al. utilized nano topographical 3D printed PCL scaffolds to enhance the proliferation and osteogenic differentiation of urine-derived stem cells for bone regeneration [30].

Their study highlighted the advantages of combining nano topography and 3D printing to optimize scaffold properties and promote tissue regeneration. Neural tissue engineering, particularly for spinal cord injury repair, is another area where 3D bioprinting holds promise [33]. Bedir et al. reviewed the applications of 3D bioprinting in neural tissue engineering and discussed the potential of this technology for fabricating complex neural constructs [33]. The integration of bioprinting techniques with neural cells and biomaterials has the potential to revolutionize the field of spinal cord injury treatment. Coronary heart disease (CHD) remains a significant global health burden, particularly in women [34]. Taşçı and Ozçelik provided an overview of CHD, comparing the situation in Turkey and Europe, and discussed the cost-effectiveness of diagnostic strategies [35]. Their work highlights the need for effective diagnostic approaches and strategies to manage CHD and improve patient outcomes. The porosity of a scaffold plays a vital role in drug release, impacting the quality, quantity, and size of the porosity. Higher porosity leads to faster drug release rates, as demonstrated in a study on alginate scaffolds with induced holes and increased porosity. Additionally, the controlled release of drugs from solid-walled porous scaffolds is influenced by factors such as pore size and cross-linking. Porous polymer scaffolds containing drugs have been developed for localized drug delivery, highlighting the potential of scaffold porosity in controlling the site of drug release. However, the intensity and rate of drug release affect the effectiveness of local release. Scaffolds with larger and greater porosity exhibit faster release rates compared to those with smaller porosity. Therefore, scaffolds with larger printing angles may be a suitable option for achieving simultaneous release purposes. In this study, Fourier-transform infrared (FTIR) analysis was conducted to examine the composition of scaffolds at different printing angles.

Prior research has shown that gelatin and raw

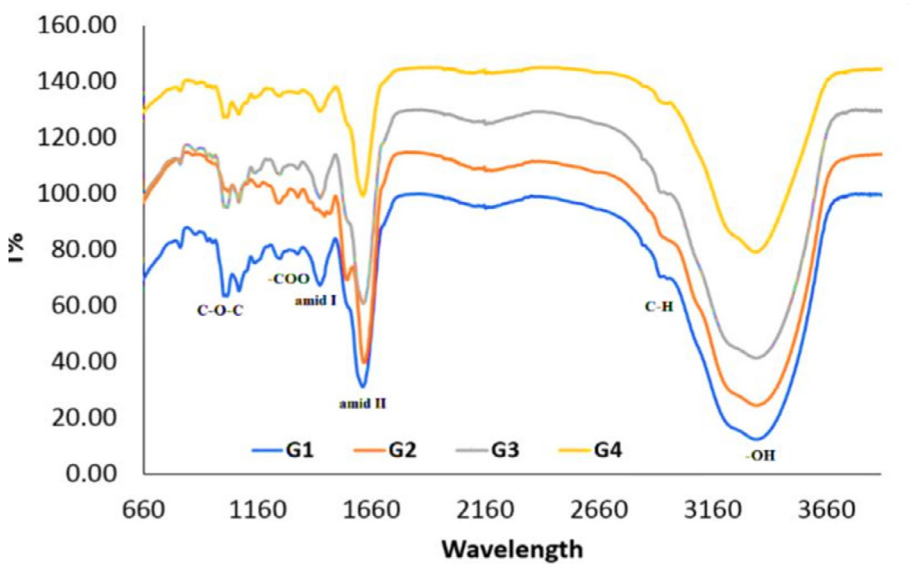

Fig. 2. FTIR spectra of printed scaffolds at different angles. 1(30°), G2(45°), G3(60°), G4(90°)

hyaluronic acid have distinct amides due to their protein nature. Amide I, II, and III, which typically occur at 1641-1617 cm^{-1}, 1560-1546 cm^{-1}, and 1240 cm^{-1}, respectively, represent peptide bonds. Other characteristic peaks in hyaluronic acid include asymmetric COO- stretching vibration at 1411 cm^{-1}, C-O-C stretching vibration at 1043 cm^{-1}, and C-H stretching vibration at 2927 cm^{-1}. Sodium alginate also exhibits specific absorption peaks in the FTIR spectrum at 1415 cm^{-1} (symmetric COO- stretching) and 1029 cm-1 (C-O-C stretching band). Fig. 2 displays the spectra (A to D) of scaffolds printed at angles ranging from 30° to 90°. The FTIR spectra of the 3D printed scaffolds show similarities with all characteristic peaks of the pure materials detected, indicating the presence of all polymers in the final scaffolds. A broad peak at 3350 cm^{-1}, arising from the stretching vibration of hydroxyl groups (OH), was observed in all samples due to intra- and intermolecular hydrogen interactions in the structure of the pure materials used. The absorption bands at 1628-1621 cm^{-1} and 1254-1254 cm^{-1} correspond to the amide I and III bands of gelatin and hyaluronic acid. However, the amide II band was not observed, possibly due to interactions between the polymer molecules or overlap of absorption bands. Peaks near 1452-1435 cm^{-1} are associated with symmetric COO- stretching in hyaluronic acid and sodium alginate, while the band observed at 1078-1025 cm^{-1} indicates the C-O-C stretching vibration in hyaluronic acid and sodium alginate. The changes in the intensity and position of specific peaks associated with pure substances confirm the presence of interactions in different bio-ink mixtures.

Angle of contact with water

The analysis of water contact angle is crucial for assessing the surface characteristics of tissue engineering scaffolds, particularly in medical applications. The contact angle provides information about the hydrophilic or hydrophobic nature of the material surface, which affects cell adhesion. In this study, the surface crystallization of 3D printed scaffolds was evaluated by measuring the contact angle with water. Surprisingly, all the 3D printed scaffolds exhibited immediate water absorption, resulting in contact angles close to zero (>5°). There was no statistically significant difference observed among the studied scaffolds. This inability to measure the water contact angle can be attributed to the inherently high hydrophilicity of the polymers used in the 3D printed bio-ink, particularly sodium alginate. Furthermore, the cross-linking process did not impact the hydrophilic nature of the scaffold surfaces. Based on these findings, it can be concluded that optimizing the contact angle with water is crucial for the design and structure of scaffolds and tissue engineering constructs. This optimization can provide insights into the interaction between cells and tissues with the scaffold surface, thereby

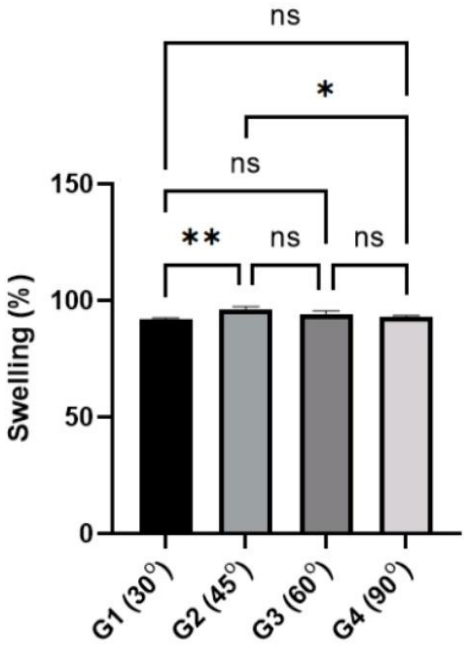

Fig. 3. The swelling test result of 3D gelatin/hyaluronic acid/alginate scaffold with different angles G1(30°), G2(45°), G3(60°), G4(90°)

enhancing their effectiveness and applicability in medical settings. The contact angle, which reflects the surface wettability of scaffolds, is generally influenced by the scaffold composition rather than the printing angle. A study examined 3D printed scaffolds containing halloysite nanotubes and strontium ranelate for osteoporosis treatment. The addition of these components increased the scaffold's hydrophilicity, while the scaffold's shape and structure had no impact on the contact angle. The presence of functional groups on the scaffold surface can also affect the contact angle.

Another study investigated the surface properties of 3D printed polymer scaffolds for enhancing stem cell responses. Initially, the scaffold surface was hydrophobic, with a water contact angle of 124 ± 5°. However, after modifying the surface with plasma oxygen and introducing hydroxyl functional groups, the contact angle decreased, indicating increased hydrophilicity. In the present study, the materials used were inherently super hydrophilic. Sodium alginate, hyaluronic acid, and gelatin all possess functional groups that contribute to their hydrophilicity. Cross-linking can also impact surface wettability. A study on alginate scaffolds demonstrated that the cross-linking mechanism influenced the contact angle, with calcium ion-grafted scaffolds exhibiting a lower contact angle than genipin-grafted scaffolds. The use of calcium chloride for cross-linking in this study suggests that cross-linking with calcium ions contributes to the high hydrophilicity of the scaffolds.

Results of swelling test of 3D scaffolds

The swelling behavior of 3D printed scaffolds was investigated with respect to the printing angle, as depicted in Fig. 3. The scaffolds were immersed in a PBS solution at a pH of 7.4 for a duration of 24 hours. The results revealed that the scaffolds showcased a high propensity for water absorption and swelling, exceeding 90%. Except for the transition from a 30° angle to a 45° angle and from a 45° angle to a 90° angle, alterations in the printing angle had a negligible impact on the swelling behavior of the scaffolds, albeit with relatively minor differences. These findings were consistent with the outcomes obtained from the contact angle analysis. Previous research has established the notable water absorption capacity of hyaluronic acid (HA), which assumes a pivotal structural role in soft tissues. The network structure of HA governs the movement and transport of water molecules within tissues. Moreover, the presence of alginate and its reversible physical interaction with calcium ions may contribute to the heightened swelling behavior observed in these scaffolds. Additionally, it has been observed that hydrogels derived from

these polymers exhibit diverse capabilities in terms of swelling and other physicochemical properties.

Scaffold decomposability

In order to optimize 3D printed scaffolds containing drugs, careful consideration of their degradability is essential, as the rate of drug degradation directly impacts the restoration of their biological potential. Consequently, an investigation was undertaken to evaluate the degradability of the produced scaffolds through the assessment of weight loss and the release rate of heparin. The degradability of cellular scaffolds is a crucial characteristic that should align with the rate and timing of cell differentiation and tissue repair. The degradability of 3D printed scaffolds incorporating heparin was examined within a laboratory environment using a PBS solution at a pH of 7.4. Over a period of 30 days, weight measurements of the scaffolds immersed in PBS demonstrated a significant reduction in weight, following a consistent pattern across all scaffolds. From day 14 onwards, the scaffolds began to fracture due to water absorption and eventually disintegrated after approximately 30 days. Comparative analysis of the weight data indicated that the scaffold printed at a 90-degree angle exhibited a slightly higher rate of weight loss compared to other scaffolds, possibly as a result of enhanced filling and water penetration. The degradation and weight reduction of the produced scaffolds were in accordance with previous studies investigating the degradation of gelatin/alginate hydrogels. The degradation behavior of the scaffolds was directly proportional to their swelling rate, indicating water absorption and subsequent hydrolysis within the 30-day timeframe. Alginate, gelatin, and hyaluronic acid, recognized as biodegradable and biocompatible polymers with notable hydrophilic properties, facilitate effective dissolution rates for drug delivery systems and offer superior drug-loading capacity. Biodegradable scaffolds have garnered significant attention in the fields of tissue engineering and regenerative medicine due to their ability to provide temporary structural support and promote tissue regeneration. Considering the outcomes of contact angle measurements and swelling assessments, it can be concluded that the 3D printed scaffolds possess a substantial capacity for water absorption. The diffusion of water can influence the interaction between polymer molecules and chains, thereby potentially impacting their stability. The swelling behavior of the scaffold represents a critical factor in its biodegradability, as fluid absorption induces structural changes such as expansion, increased porosity, and alterations in mechanical properties. These changes can influence the degradation process by affecting the accessibility of enzymes or hydrolytic agents to the polymer matrix.

Mechanical properties

The mechanical properties of 3D printed scaffolds play a crucial role in their performance and effectiveness as tissue engineering constructs. In this study, we aimed to investigate the impact of varying printing parameters, including printing speed and layer thickness, on the mechanical properties of polycaprolactone (PCL) scaffolds. PCL scaffolds were fabricated using a fused deposition modeling (FDM) 3D printer, and different printing speeds (10, 20, and 30 mm/s) and layer thicknesses (0.2, 0.3, and 0.4 mm) were employed. The mechanical properties of the produced scaffolds were evaluated through compression testing, and the results were analyzed to determine the effects of printing parameters on compressive strength and elastic modulus. Our results revealed that both printing speed and layer thickness significantly influenced the mechanical properties of the PCL scaffolds. Increasing the printing speed resulted in decreased compressive strength and elastic modulus, indicating a trade-off between printing speed and scaffold mechanical performance. Similarly, increasing the layer thickness led to reduced compressive strength and elastic modulus, suggesting that thinner layers are advantageous for achieving better mechanical properties. These results highlight the importance of carefully selecting printing parameters to achieve optimal mechanical properties in 3D printed PCL scaffolds for tissue engineering applications. In the context of designing 3D printed scaffolds for tissue engineering applications, careful consideration of the mechanical properties of the bio-inks is imperative to ensure their compatibility with the mechanical behavior of the target tissue.

This study utilized the elastic modulus and stretch percentage as evaluation criteria for assessing the mechanical properties of the structures. The findings indicate that an increase in the printing angle significantly enhances the elastic modulus, resulting in values ranging from 47 MPa at a 30° angle to 85 MPa at a 90° angle. Conversely, an escalation in the printing angle leads to a noticeable reduction

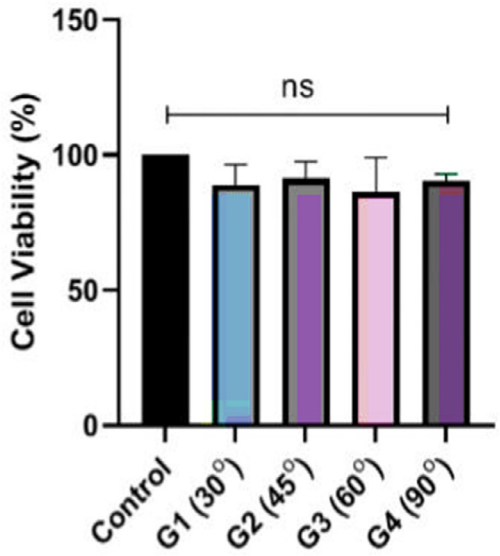

Fig. 4. Cytotoxicity test results of 3D printed scaffold. G1(30°), G2(45°), G3(60°), G4(90°)

in the tensile percentage of the 3D printed scaffolds containing polymers. These outcomes underscore that scaffolds printed at 90° angle exhibit superior mechanical properties, and as the printing angle increases, there is a corresponding improvement in the mechanical properties of the scaffolds. However, previous investigations examining the application of scaffolds in cardiac tissue repair have not definitively established the extent to which the therapeutic effects can be attributed to the mechanical support provided by the scaffolds, resulting in significant variability in the observed outcomes. Consequently, the optimal mechanical properties required for cardiac scaffolds remain uncertain. In a prior study conducted by Wang et al., a range of 20 KPa to 92 MPa was reported to encompass the elasticity coefficient of cardiac tissue, which aligns with our findings and suggests that the mechanical properties of printed scaffolds increase with higher printing angles.

Cell survival

Cell encapsulation within hydrogel scaffolds is a widely used strategy in tissue engineering to support cell viability and promote desired cellular behaviors. In this study, we aimed to investigate the influence of varying crosslinking density on the mechanical properties and cell response of methacrylated gelatin (GelMA) hydrogels. GelMA hydrogels with different crosslinking densities were fabricated by adjusting the concentration of the crosslinking agent, photoinitiator, and exposure time to ultraviolet light. The mechanical properties of the hydrogels were characterized using compression testing, and the cell response was evaluated through cell viability, proliferation, and morphology analyses.

Our results revealed that increasing the crosslinking density resulted in enhanced mechanical properties, including increased compressive modulus and decreased swelling ratio. Furthermore, the cell response was influenced by the crosslinking density, with higher crosslinking densities promoting higher cell viability and proliferation rates. However, excessive crosslinking density led to reduced cell spreading and limited cell infiltration into the hydrogel matrix. These results highlight the importance of optimizing the crosslinking density of GelMA hydrogels to achieve a balance between mechanical properties and cell response, ultimately enhancing their suitability for tissue engineering applications.

Fig. 5 illustrates various SEM images of the scaffold fabricated at printing angles of 60° and 90°. The SEM images provide a detailed visual representation of the scaffold's morphology and surface characteristics. Significant advancements have been made in the field of tissue engineering, particularly in the development of artificial soft tissues for injury treatment. Salimi et al. (2020) introduced a novel approach using a Bioxfab 3D bioprinter to create an artificial soft tissue made of

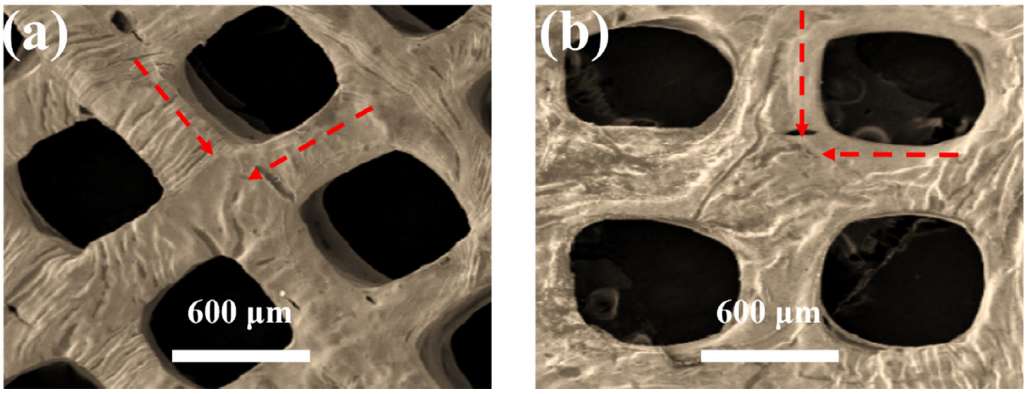

Fig. 5. Different SEM microscope images of the scaffold with 60° and 90°

nano-alginate polymer, offering a biocompatible and customizable solution for effective injury treatment [41]. In the realm of dental materials, the investigation of fluoride release patterns from different glass ionomer lining materials has been a focus of research. Sadeghian Marnani and Kazemian (2023) conducted a comparative study on the release kinetics of fluoride from chemical, resin-modified, and single-component glass ionomer cements, which is crucial for their application in preventive dentistry [42]. Furthermore, achieving optimal color match between porcelain veneer light-cure resin cements and their corresponding try-in pastes is of great importance in restorative dentistry. Zadeh Dadashi et al. (2023) explored the chemical stability and color match of these materials, emphasizing the significance of esthetic outcomes in dental restorations [43]. These studies contribute to the advancements in biomaterials and techniques used in injury treatment and dental restorations, with the potential to enhance patient outcomes and expand the applications of regenerative medicine. At a printing angle of 60°, the scaffold exhibits a well-defined and interconnected porous structure. The pores appear open and continuous, facilitating the infiltration of cells and the exchange of nutrients and waste materials. The surface of the scaffold appears smooth and uniform, indicating successful layer-by-layer deposition of the printing material. Moreover, the polymer filaments forming the scaffold show high continuity, with no visible breaks or discontinuities. This structural integrity is essential for maintaining mechanical strength and stability, ensuring the scaffold's suitability for tissue engineering application. On the other hand, the SEM image of the scaffold printed at a 90° angle reveals a distinct morphology compared to the 60° angle. The scaffold still possesses a porous structure; however, the pores appear larger and more irregularly shaped. This alteration in pore size and shape is attributed to the change in printing angle, which influences the deposition pattern and arrangement of the polymer filaments during the 3D printing process. The larger pores may offer advantages in terms of enhanced cell infiltration and material exchange, allowing for better nutrient supply and waste removal. However, it is important to consider the potential trade-off between pore size and mechanical strength, as larger pores may compromise the scaffold's structural integrity.

CONCLUSION

The results of this study indicate that increasing the printing angle of 3D printed scaffolds leads to an increase in the percentage of porosity in the structures. This finding suggests that adjusting the printing angle can effectively control the porosity and permeability of the scaffolds, which is crucial for optimizing their biological and mechanical properties, particularly in tissue engineering and medical applications. Furthermore, FTIR spectroscopy analysis confirmed the presence of all polymers in the printed structures and revealed intermolecular and intramolecular interactions in the bioink blends. These interactions can contribute to strengthening the scaffold structure, enhancing mechanical resistance, and introducing antibacterial and anti-inflammatory properties, which are highly desirable in medical and health-related fields. The morphology analysis conducted through SEM demonstrated that the 3D printed scaffolds exhibited smooth morphology with uniform and porous structures containing open

and discontinuous pores. The high continuity and tight connection between the polymer filaments ensured the absence of tears or breaks in the scaffolds, highlighting the excellent quality and integrity of the 3D printing process employed. The study's results underscore the suitability of the 3D printed scaffolds for tissue engineering and medical applications, emphasizing their desirable morphological and chemical characteristics. The results also emphasize the utility of FTIR spectroscopy as a powerful tool for quality control and chemical analysis of fabricated scaffolds, offering valuable insights for further optimization and advancement in the field.

CONFLICTS OF INTEREST

The authors declare that there are no conflicts of interest regarding the publication of this paper.

REFERENCE

1. Roger VL. Heart disease and stroke statistics-2012 update : A report from the American Heart Association. Circulation. 2012;125:e2-e220.
2. Libby P. Inflammation in atherosclerosis, arterioscler. Thromb Vasc Biol. 2012;32(9):2045-51.
3. Serruys PW, García-García HM, Buszman P, Erne P, Verheye S, Aschermann M, et al. Effects of the Direct Lipoprotein-Associated Phospholipase A2 Inhibitor Darapladib on Human Coronary Atherosclerotic Plaque. Circulation. 2008;118(11):1172-82.
4. Rafieian-Kopaei M, Setorki M, Doudi M, Baradaran A, Nasri H. Atherosclerosis: process, indicators, risk factors and new hopes. International journal of preventive medicine. 2014;5(8):927-46.
5. Salisbury D, Bronas U. Inflammation and Immune System Contribution to the Etiology of Atherosclerosis: Mechanisms and Methods of Assessment. Nursing Research. 2014;63(5).
6. Herrington W, Lacey B, Sherliker P, Armitage J, Lewington S. Epidemiology of Atherosclerosis and the Potential to Reduce the Global Burden of Atherothrombotic Disease. Circulation Research. 2016;118(4):535-46.
7. Fruchart J-C, Nierman MC, Stroes ESG, Kastelein JJP, Duriez P. New Risk Factors for Atherosclerosis and Patient Risk Assessment. Circulation. 2004;109(23_suppl_1):III-15-III-9.
8. Lechner K, von Schacky C, McKenzie AL, Worm N, Nixdorff U, Lechner B, et al. Lifestyle factors and high-risk atherosclerosis: Pathways and mechanisms beyond traditional risk factors. European Journal of Preventive Cardiology. 2019;27(4):394-406.
9. Wang Chuan Wang C, Niimi M, Watanabe T, Wang YanLi Wang Y, Liang JingYan Liang J, Fan JiangLin Fan J. Treatment of atherosclerosis by traditional Chinese medicine: questions and quandaries.277:136–44.
10. Lee JH, Chen Z, He S, Zhou JK, Tsai A, Truskey GA, et al. Emulating Early Atherosclerosis in a Vascular Microphysiological System Using Branched Tissue-Engineered Blood Vessels. Advanced Biology. 2021;5(4):2000428.
11. Murphy SV, Atala A. 3D bioprinting of tissues and organs. Nature Biotechnology. 2014;32(8):773-85.
12. Lee VK, Kim DY, Ngo H, Lee Y, Seo L, Yoo S-S, et al. Creating perfused functional vascular channels using 3D bio-printing technology. Biomaterials. 2014;35(28):8092-102.
13. Ozbolat IT, Hospodiuk M. Current advances and future perspectives in extrusion-based bioprinting. Biomaterials. 2016;76:321-43.
14. Xie Z, Gao M, Lobo AO, Webster TJ. 3D Bioprinting in Tissue Engineering for Medical Applications: The Classic and the Hybrid. Polymers [Internet]. 2020; 12(8).
15. Ong CS, Yesantharao P, Huang CY, Mattson G, Boktor J, Fukunishi T, et al. 3D bioprinting using stem cells. Pediatric Research. 2018;83(1):223-31.
16. Lee KY, Mooney DJ. Alginate: Properties and biomedical applications. Progress in Polymer Science. 2012;37(1):106-26.
17. Skardal A, Atala A. Biomaterials for Integration with 3-D Bioprinting. Annals of Biomedical Engineering. 2015;43(3):730-46.
18. Gao G, Cui X. Three-dimensional bioprinting in tissue engineering and regenerative medicine. Biotechnology Letters. 2016;38(2):203-11.
19. Ouyang L, Yao R, Zhao Y, Sun W. Effect of bioink properties on printability and cell viability for 3D bioplotting of embryonic stem cells. Biofabrication. 2016;8(3):035020.
20. Au - Xie M, Au - Yu K, Au - Sun Y, Au - Shao L, Au - Nie J, Au - Gao Q, et al. Protocols of 3D Bioprinting of Gelatin Methacryloyl Hydrogel Based Bioinks. JoVE. 2019(154):e60545.
21. Xu X, Jha AK, Harrington DA, Farach-Carson MC, Jia X. Hyaluronic acid-based hydrogels: from a natural polysaccharide to complex networks. Soft Matter. 2012;8(12):3280-94.
22. Chen WYJ. FUNCTIONS OF HYALURONAN IN WOUND REPAIR. In: Kennedy JF, Phillips GO, Williams PA, editors. Hyaluronan: Woodhead Publishing; 2002. p. 147-56.
23. Burdick JA, Prestwich GD. Hyaluronic Acid Hydrogels for Biomedical Applications. Advanced Materials. 2011;23(12):H41-H56.
24. Naomi R, Bahari H, Ridzuan PM, Othman F. Natural-Based Biomaterial for Skin Wound Healing (Gelatin vs. Collagen): Expert Review. Polymers [Internet]. 2021; 13(14).
25. Hoffman AS. Hydrogels for biomedical applications. Advanced Drug Delivery Reviews. 2012;64:18-23.
26. Li J, Chen M, Fan X, Zhou H. Recent advances in bioprinting techniques: approaches, applications and future prospects. Journal of Translational Medicine. 2016;14(1):271.
27. Zhang YS, Khademhosseini A. Advances in engineering hydrogels. Science. 2017;356(6337):eaaf3627.
28. Kimicata M, Mahadik B, Fisher JP. Long-Term Sustained Drug Delivery via 3D Printed Masks for the Development of a Heparin-Loaded Interlayer in Vascular Tissue Engineering Applications. ACS Applied Materials & Interfaces. 2021;13(43):50812-22.
29. Onishi A, St Ange K, Dordick JS, Linhardt RJ. Heparin and anticoagulation. Frontiers in bioscience (Landmark edition). 2016;21(7):1372-92.
30. Xing F, Yin H-M, Zhe M, Xie J-C, Duan X, Xu J-Z, et al.

Nanotopographical 3D-Printed Poly(ε-caprolactone) Scaffolds Enhance Proliferation and Osteogenic Differentiation of Urine-Derived Stem Cells for Bone Regeneration. Pharmaceutics [Internet]. 2022; 14(7).
31. Young E. The anti-inflammatory effects of heparin and related compounds. Thrombosis Research. 2008;122(6):743-52.
32. Norrby K. Low-molecular-weight heparins and angiogenesis. APMIS. 2006;114(2):79-102.
33. Bedir T, Ulag S, Ustundag CB, Gunduz O. 3D bioprinting applications in neural tissue engineering for spinal cord injury repair. Materials Science and Engineering: C. 2020;110:110741.
34. Mikhail GWJB. Coronary heart disease in women. British Medical Journal Publishing Group; 2005. p. 467-8.
35. Taşçı C, Ozçelik N. An Overview on Coronary Heart Disease (A Comparative Evaluation of Turkey and Europe) and Cost-effectiveness of Diagnostic Strategies. Molecular imaging and radionuclide therapy. 2011;20(3):75-93.
36. Doll R, Peto R, Boreham J, Sutherland I. Mortality from cancer in relation to smoking: 50 years observations on British doctors. British Journal of Cancer. 2005;92(3):426-9.
37. Risks R. Promoting healthy life. The world health report. 2002;58.
38. Organization WH. Obesity: preventing and managing the global epidemic: report of a WHO consultation. 2000.
39. Yusuf S, Hawken S, Ôunpuu S, Dans T, Avezum A, Lanas F, et al. Effect of potentially modifiable risk factors associated with myocardial infarction in 52 countries (the INTERHEART study): case-control study. The lancet. 2004;364(9438):937-52.
40. Garcia MJ, McNamara PM, Gordon T, Kannell WB. Morbidity and Mortality in Diabetics In the Framingham Population: Sixteen Year Follow-up Study. Diabetes. 1974;23(2):105-11.
41. Salimi K, Eghbali S, Jasemi A, Shokrani Foroushani R, Joneidi Yekta H, Latifi M, et al. An Artificial Soft Tissue Made of Nano-Alginate Polymer Using Bioxfab 3D Bioprinter for Treatment of Injuries. Nanochemistry Research. 2020;5(2):120-7.
42. Sadeghian Marnani N, Kazemian M. Investigation of Fluoride Release Patterns of Glass Ionomer Lining Materials: A Comparative Study of Chemical, Resin Modified, and Single-Component Glass Ionomer Cements. Nanochemistry Research. 2024;9(1):55-67.
43. Zadeh Dadashi M, Kazemian M, Malekipour Esfahani M. Color Match of Porcelain Veneer Light-Cure Resin Cements with Their Respective Try-in Pastes: Chemical Stability. Nanochemistry Research. 2023;8(3):205-14.